

1  
2  
3     **Composite pH-sensitive cryogels for dual drug delivery and enhanced mechanical**  
4  
5     **properties**  
6  
7

8     Gabriel G. de Lima<sup>1</sup>, Fanny Traon<sup>1</sup>, Elouan Moal<sup>1</sup>, Maria Canillas<sup>2</sup>, Miguel A. Rodriguez<sup>2</sup>,  
9  
10    Nicholas Dunne<sup>3-5</sup>, Declan M. Devine<sup>1,6</sup>, \*Michael J.D. Nugent<sup>1</sup>  
11  
12

13    <sup>1</sup> Materials Research Institute, Athlone Institute of Technology, Athlone, Ireland  
14  
15    <sup>2</sup> Ceramic and Glass Institute from CSIC, Madrid, Spain.  
16

17    <sup>3</sup> School of Pharmacy, Queen's University, Belfast, 97 Lisburn Road, BT9 7BL, United  
18  
19    Kingdom  
20

21    <sup>4</sup> Centre for Medical Engineering Research, School of Mechanical and Manufacturing  
22  
23    Engineering, Dublin City University, Stokes Building, Collins Avenue, Dublin 9, Ireland  
24

25    <sup>5</sup> Trinity Centre for Bioengineering, Trinity Biomedical Sciences Institute, Trinity College  
26  
27    Dublin, Dublin 2, Ireland  
28

29    <sup>6</sup> Rehabilitation Medicine Centre, Mayo Clinic, Rochester, MN, USA.  
30  
31

32    \*Corresponding author. Tel: +353 9064 68172; fax: +353 0964 68148; e-mail address:  
33  
34    mnugent@ait.ie  
35  
36  
37  
38  
39  
40  
41  
42  
43  
44  
45  
46  
47  
48  
49  
50  
51  
52  
53  
54  
55  
56  
57  
58  
59  
60

**ABSTRACT**

In this study, we present a simple and effective process that integrates hydrogels with drugs + ceramics via physical crosslinks resulting in improved mechanical properties. These cryogels have the potential for controlled drug release and stimulus responsive behaviour. The hydrogels were produced from polyvinyl alcohol and polyacrylic acid by varying the molecular weight of the polymers, via freeze thawing technique. The cryogels were combined with two ceramics: (1) a combination of beta-tricalcium phosphate, wollastonite, magnesium silicate and (2) titanium dioxide nanopowder. Theophylline, a model drug, was incorporated into the structure to analyse the drug release behaviour. A layered structure was produced by adding both hydrogels + ceramics into a mould where a polyvinyl alcohol dried film acted as a barrier and reinforcing structure. The results showed that the barrier integrated between both hydrogels by a physically crosslinking mechanism. This adhesion was demonstrated using Fourier transform infrared spectroscopy and scanning electron microscopy. Swelling of this composite showed the profile of drug release from both hydrogels + ceramics while simultaneously releasing the drug independently without diffusing via the opposite layer. Finally, mechanical properties were improved with the addition of the ceramics, which demonstrates the potential approach in terms of modification of weak hydrogel systems.

## 1 2 3 4 5 6     **1. Introduction**

7  
8  
9  
10  
11  
12  
13  
14  
15  
16  
17  
18  
19  
20  
21  
22  
23  
24  
25  
26  
27  
28  
29  
30  
31 Polyvinyl alcohol (PVA) is a synthetic biocompatible polymer that is able to form physical or  
32 chemical crosslinking based on different methods such as UV-irradiation [1,2] or freeze-  
33 thawing [3–5]. Freeze thawing PVA hydrogels are a good alternative for producing  
34 biomedical composites [6,7] or drug delivery devices [6–8] because the process does not  
35 contain any solvent or other components that can increase the overall toxicity. Freeze-thawed  
36 hydrogels are formed upon freezing the solubilised polymer, and physical crosslinking occurs  
37 via hydrogen bonding based on the ice crystals growth [9,10]. The interesting aspect of freeze-  
38 thawed hydrogels is that they can be moulded into any kind of device or structure [11],  
39 changing their properties is largely dependent on the number of freeze-thaw (F/T) cycles  
40 [12], and for this, it can show useful properties for biomedical applications, such as memory-  
41 shape [13,14] or self-healing [15,16] properties.

42  
43  
44  
45  
46  
47  
48  
49  
50  
51  
52  
53  
54  
55  
56  
57  
58  
59  
50 PVA, produced by freeze-thawing, or cryogels, can also hold in its structure numerous  
51 materials that can enhance their properties, for example mechanical [17], swelling [18,19],  
52 controlled drug delivery [20] and pH- [7], pressure- [21] or temperature-sensitive [22].  
53 Polyacrylic acid, PAA, can improve the pH sensitivity for drug delivery applications [19].  
54 Furthermore, the addition of ceramics into the structure can improve its mechanical  
55 properties. Our group studied the incorporation of ceramics containing beta-tricalcium  
56 phosphate ( $\beta$ -TCP) into the structure of PVA-PAA cryogels, which reinforce the structure  
57 and can target deliver a drug acting as anti-infect barrier [23].

58  
59  
60  
58 The incorporation of two or more different drugs into the same hydrogel structure can  
59 decrease its properties and exhibit a very challenging behaviour [24]. The combination of  
60 various drugs with different therapeutic effects has gathered much interest recently, since it  
can potentially treat infections and accelerate the tissue healing process. However, one of the

major challenges is how to reliably control the release of each drug independently [25]. A simple method for dual delivery without affecting the mechanical properties of the polymer is to use layered hydrogels [25,26]. A similar technique has been performed by Yang [27], which utilised a double layered hydrogel PVA, with chitosan and glycerol with one layer produced by freeze-thawing following by UV-irradiation and another layer with only UV-irradiation, this technique incorporated both properties of the F/T and UV-irradiation. The solubilised polymer, submitted to UV-irradiation only, is built on top of the PVA hydrogel prepared by F/T and diffuses towards it. This results in chemical crosslinking in both layered polymers. However, since there is spreading of the solution onto the other layer, this can be a problem if each layer is carrying different drugs and is targeted for drug delivery.

The work proposed in the current study is a simple and effective way to produce layered hydrogels that can incorporate different ceramics + drugs, which act independently while also forming physical crosslinks between the separate layers. Therefore, this work investigated the application of polymeric/ceramic bilayer composites comprising of PVA and PAA as the polymer matrix to provide pH sensitivity, swelling capability and carrier vehicle for the drugs. In addition, two different ceramic materials were incorporated in two layers: (1) –  $\beta$ -TCP to support enhanced mechanical properties [28,29] and (2) titanium dioxide ( $TiO_2$ ) to provide a controlled drug release. [30]. The construct was produced by introducing a PVA dried hydrogel, xerogel, produced by freeze-thawing in the division of both solubilised polymers + oxides following five F/T. Theophylline was incorporated into each layer to evaluate the drug release profile.

## 2. Materials and Methods.

### 2.1 Materials

PVA, PAA, theophylline, Phosphate Buffer Saline (PBS) and TiO<sub>2</sub> rutile nanopowder <100 nm were supplied by Sigma-Aldrich, Ireland. Tricalcium phosphate (TCP) supplied from Carlo Erba, Italy, Wollastonite (W) NYAD® 1250 from NYCO®, and Talc were supplied by Sigma-Aldrich, Spain.

## 2.2 Ceramic fabrication

Ceramic grains were obtained using the procedure previously described [23]. Briefly, an initial composition of 60% TCP, 25% W, and 15% Talc (wt.%) were mixed for 1 h at 60 °C. The powder blend was then grounding using a tungsten mortar and sieved to a size ≤100 μm. The selected powders were compacted at 1,000 kPa/cm<sup>2</sup> during 60 s using uniaxial press and sintered at 1050 °C for 2 h. Grains were reground and sieved to particle size ranging between 45 μm and 100 μm. Thereafter the powder was subjected to further compaction (1,000 kPa/cm<sup>2</sup>) and then sintered at 1050°C for 2 h. The final stage involved regrinding the powder grains and further sieving to a particle size distribution of 100 μm to 300 μm. The ceramics obtained on completion of the thermal treatment process were β-TCP, where Ca<sup>2+</sup> is partially substituted with Mg<sup>2+</sup> (Ca<sub>2.81</sub>Mg<sub>0.19</sub>(PO<sub>4</sub>)<sub>2</sub>), wollastonite 2M (CaSiO<sub>3</sub>) and traces of Enstatite (Mg<sub>2</sub>Si<sub>2</sub>O<sub>6</sub>).

## 2.3 Polymeric-ceramic composition formulation and fabrication of composites

Physically crosslinked hydrogels were prepared by dissolving known concentrations of PVA, with average molecular weight of 195,000 and a percentage of hydrolysis of 98% (Mowiol 56-98) at 5% concentration (w/v) in distilled water (dH<sub>2</sub>O), at 80 °C with constant stirring until the complete solubilisation of PVA was achieved. Subsequently, ceramic grains were dispersed in the polymer solution at either or 75 (wt.%) of PVA, and finally PAA with molecular weight of 450,000 (labelled as paa in our work) and 3,000,000 (labelled as PAA in

1  
2 our work) at concentration of 50% (w/w) of the PVA weight were added to the solution at  
3 ambient temperature.  
4  
5

6  
7 Finally, the samples were rapidly frozen to constant temperature of -80 °C for 2 h using an  
8 ultra-low temperature freezer (Innova U535 ultra-low temperature freezer; New Brunswick  
9 Scientific, Edison, NJ). The frozen solutions were then thawed in a controlled temperature  
10 environment of 25 °C.  
11  
12

13 To produce the bilayer hydrogels - Fig. 1 exemplifies the process. PVA containing β-TCP  
14 was added into one side of the mould and PVA containing TiO<sub>2</sub> rutile on the other side. The  
15 PVA containing ceramics were subjected to one F/T cycle before linking together. One F/T  
16 cycle was used, as this increases the crosslink in the structure but not at the point to form a  
17 strong gel, rather leading to a viscous and weak gel. The central xerogel was produced by five  
18 F/T cycles. Two geometries were produced as shown in Fig. 1. After the assembly of the  
19 polymers into the mould, they were rapidly frozen and thawed, this procedure was replicated  
20 four times. An oven (Genlab thermal, MINO/50, UK) was used for 24 h at 30 °C to remove  
21 the water from the hydrogels until the samples were completely dried.  
22  
23

#### 24 2.4 Scanning electron microscopy (SEM) 25 26

27 Composite morphology was observed using a Tescan mira XMU scanning electron  
28 microscope (SEM, TESCAN, Brno, CZ) in back scattered electron (BSE) mode using  
29 magnifications, which ranged from 50-500x. Prior to scanning the samples were sliced to  
30 obtain cross-sectional regions. The samples also were sputtered with a gold using Baltec SCD  
31 005 for 110 s at 0.1 mBar vacuum before testing yielding a coating of approximately 110 nm.  
32  
33

#### 34 2.5 Attenuated total reflectance Fourier transform infrared spectroscopy (ATR-FTIR) 35 36

37 Attenuated total reflectance Fourier transform infrared spectroscopy (FTIR) was conducted  
38 using a Perkin Elmer (Spectrum One FT-IR Spectrometer, Perkin Elmer Instrument, USA)  
39  
40

1  
2 spectrometer fitted with a universal ATR sampling accessory. All data was recorded in the  
3 spectral range of 4000–520 cm<sup>-1</sup> utilising a four scan per sample cycle at a resolution of 0.5  
4 cm<sup>-1</sup>.  
5  
6  
7  
8  
9

10 2.6 Kinetics of hydrogels  
11  
12

13 Swelling studies of the composite samples were conducted in PBS at pH 7.4. For the swelling  
14 properties, the PVA hydrogels was measured gravimetrically. To measure the swelling  
15 kinetics, the pre-weighted samples were immersed in PBS. Periodically samples were  
16 removed and the excess surface solution was gently removed with paper towel and the  
17 swollen samples were weighted at various time intervals. The swelling ratio percentage of a  
18 hydrogel can be defined as:  
19  
20  
21  
22  
23  
24  
25

$$26 S(\%) = \frac{(W_s - W_d)}{W_d} \times 100 \quad (1)$$

27  
28

29 where S (%) represents the weight of the swollen hydrogel at an specific time, also known as  
30 water uptake content, and W<sub>d</sub> is the hydrogel dried mass before beginning the swelling  
31 studies. Samples were removed after reaching full swelling capacity on pH 7.4.  
32  
33  
34  
35  
36

37 To analyse the drug release, theophylline powder of 5 wt.% was added to the hydrogels, and  
38 solubilisation at room temperature prior to the F/T process. Drug dissolution profiles were  
39 obtained using a Distek 2100B (Distek Inc., Monmouth Junction, NJ, USA). The  
40 theophylline loaded hydrogels with were tested immediately after the F/T cycles in PBS of  
41 pH 7.4 at 37 °C. The rate of stirring was set to 100 rpm with 900 mL of dissolution media  
42 used per vessel. Three vessels were used for each scan. Aliquot volume of 4 mL was  
43 withdrawn at regular intervals and replaced with fresh buffer. After filtration, samples were  
44 manually taken at set intervals and analysed by ultraviolet (UV) light on a Perkin Elmer  
45 lambda 2 spectrometer. The % cumulative drug release was determined from the standard  
46 calibration curve of theophylline.  
47  
48  
49  
50  
51  
52  
53  
54  
55  
56  
57  
58  
59  
60

1  
2  
3 2.7 Rheological measurements  
4  
5  
6  
7  
8  
9  
10  
11  
12  
13  
14  
15  
16  
17  
18  
19  
20  
21  
22

Rheology tests were conducted using an AR 1000 rheometer (TA Instruments, Inc., Newcastle, DE, USA) from TA instruments. Frequency and strain sweeps were completed using the parallel plate method with Peltier plate temperature control. A 20 mm steel plate was used as the top geometry. A low frequency and low strain range was adopted. The frequency sweep was applied at a range of 0.1 – 100 Hz whereas the strain sweep was applied from 1.8E–04 to 1E–03 at a frequency of 1 Hz. In all cases, a compression load of  $2 \pm 0.5$  N was exerted on the swollen hydrogels during testing and data was presented as mean of two measures.

23  
24 3. Results  
25  
26  
27  
28  
29

30 3.1 Hydrogel visual inspection  
31  
32  
33  
34  
35  
36  
37  
38  
39

The hydrogel with the xerogel barrier following one cycle of F/T is exhibit in Fig.2.a. The xerogel was adhered to the composites and it was not possible to remove by normal force using the tweezers. Fig.2.b exhibits the samples following four cycles F/T, the ceramics were homogeneously dispersed throughout the PVA hydrogel and it maintained its sandwich structure following placement of the xerogel.

40  
41 2.2 Morphology  
42  
43  
44  
45  
46  
47  
48  
49  
50  
51  
52  
53  
54  
55  
56  
57  
58  
59  
60

The effect of the dried layer and interaction was investigated using the SEM to analyse the adhesion of this material. As observed in Figure 3, it is possible to observe that both ceramic and  $\text{TiO}_2$  particles were dispersed throughout the polymer structure with groups of aggregates. In addition, a porous structure occurs with variation on the pore sizes. The xerogel can be observed, indicated by arrows, and it appears to aggregate both ceramic and  $\text{TiO}_2$  particles. Although it is difficult to perceive the location of xerogel (dashed arrows in

Fig.3), its position is steady. Since the concentration used was high; the formation of agglomerates seems to be higher with the ceramics, while there are visible reductions in agglomerates in the nanopowder  $\text{TiO}_2$  portion. Furthermore, the vertical PVA xerogel (Fig.3.a) indicates a discontinuous division between the two polymers which occurs due to the difficulty on adjust the exact position of the xerogel while the dried PVA swells when preparing the samples. However, horizontal layer indicates a steadier xerogel (Fig.3.a).

### 2.3 Microstructure

The chemical structure of the different composites was obtained from a minimum of three samples - while attempting to acquire the near inter-media region between the  $\text{TiO}_2$  and  $\beta$ -TCP and is shown in Fig 4. The main peaks of PVA, PAA used in this work have been reported in literature [31], which correspond to alcohol and carboxylic acid groups. With the addition of PAA, the bands are more defined with new bands evident in the range of 1750 to 1710  $\text{cm}^{-1}$  that are due to C=O and C-O stretching of carboxylic groups [32].  $\beta$ -TCP has characteristic bands in the range of 800-1200  $\text{cm}^{-1}$  with 677 and 901  $\text{cm}^{-1}$  assigned as  $\text{SiO}_2$  with 938, 968, 1022 and 1107  $\text{cm}^{-1}$  to  $(\text{PO}_4)^{3-}$ .  $\text{TiO}_2$  main broad peak at 640  $\text{cm}^{-1}$  are characteristic of a Ti-O-Ti symmetric stretching vibration mode [33]. The incorporation of both  $\beta$ -TCP and  $\text{TiO}_2$  in the polymer is evidenced by the aforementioned peaks within the polymer structure with bands correlated to  $\beta$ -TCP and  $\text{TiO}_2$ . With the addition of PAA in both formulations, the interactions seem to be primarily with PVA as opposed to an interaction with the ceramics.

With double-layered hydrogels (Fig. 5), peaks defining the  $\beta$ -TCP and  $\text{TiO}_2$  are revealed. Although it is quite difficult to perceive the peaks when adding PAA of low M.W. but as the molecular weight increases the peaks are more defined and a strong interaction can be seen.

1  
2 Peaks of  $\beta$ -TCP are evidenced by Fig.5- black circle area. Although peaks of  $\text{TiO}_2$  are  
3 relatively weak, interaction occurs as indicated by Fig.5 in the grey circle area.  
4  
5  
6  
7  
8 2.4 Kinetics of hydrogels  
9  
10  
11 The kinetics of the hydrogels was used to understand the effects of a double composite  
12 hydrogel on drug delivery. Fig. 6 exhibits the swelling of the linked hydrogels at different  
13 times with two different configurations of the xerogel.  
14  
15  
16  
17  
18 Both samples were produced with the addition of a commercial food dye to indicate any  
19 interaction/diffusion between the xerogel and the two composites (Fig.6). After 30 min  
20 (Fig.6.c-d), a small amounts of dye spread towards the other polymer. When the maximum  
21 swelling was reached (Fig.6.e-f), the volume increases, as expected, and dye spreads a little  
22 more on both studied PVA layer conditions.  
23  
24  
25  
26  
27  
28  
29  
30 Swelling of PVA based hydrogels (Fig.7.a.) exhibits a maximum swelling ratio up to 250%.  
31 However, when the ceramics were added the values decreased in comparison to PVA. With  
32 the addition of PAA, an increase on swelling ratio occurs (Fig.7.b-c). The swelling profile of  
33 PVA + PAA composites shows slightly higher values for samples with low molecular weight  
34 of paa. Adding the ceramics had an overall decrease in swelling ratio for all profiles.  
35  
36  
37  
38  
39  
40  
41  
42 For double composite hydrogels – both PVA and PVA + PAA composites – showed swelling  
43 results as approximately the medium of the two different composites of the same proportion.  
44  
45  
46  
47 To quantify the configuration of xerogel, the swelling of the dye hydrogels of Fig.6 were also  
48 measured. The results exhibits (Fig.7.d) that horizontal layer (h) had a slower swelling ratio  
49 than samples with vertical layer (v). The dye had little effect on swelling ratio.  
50  
51  
52  
53  
54  
55 The gels utilised for drug delivery results are swollen; drug release is therefore diffusion led.  
56  
57 Drug release study (Fig.8) indicates for PVA samples a faster drug release was observed than  
58  
59  
60

for composites. For double layered hydrogels the drug release profile is dependent on the scaffold and when PAA is incorporated onto hydrogels (Fig.8.b-c), the profile for low M.W. is more dispersed when compared to PVA alone and when increasing the M.W. the drug release rate is now decreased, achieving only 30% of the drug at 6 h. This is probably due to more inter-hydrogen bonding between the PVA and PAA and the intra-molecular bonding corresponding to the ceramics.

Additionally for double layered composites with low M.W. of PAA the  $\text{TiO}_2 + \text{Drug}$  release was decreased and  $\beta\text{-TCP}$  increased this is probably because of the decreased molecular bonds leading to a more weak gel and non-controlled drug delivery. For an increased M.W. of PAA the drug release profiles are similar and no apparent differences were observed between the samples but it also had an overall slower release of the drug when compared to the other profiles.

## 2.5 Mechanical Properties

In order to understand the effect of a double layered hydrogel, samples were tested under strain-sweep and frequency sweep regimes as swollen (Fig.9). No significant differences were exhibited with PVA only samples ( $p\text{-value} > 0.05$ ) but double layered hydrogels seem to exhibit half the values of the single composites. With the addition of PAA there is a significant difference ( $p\text{-value} < 0.03$ ) between the M.W., lower M.W. reduced its values for  $\text{TiO}_2$  and it is similar for  $\beta\text{-TCP}$ . However, when the M.W. of the PAA was increased - a noticeable increase was observed.

## 4. Discussion

The focus of this work was to develop a biomedical pH sensitive PVA/PAA composite hydrogel that is able to tailor release of drug without impacting on the properties of the

1  
2 hydrogel. This study purposed a sandwich structure which maintains structural integrity  
3 between two independent polymers structure. This concept of a sandwich hydrogel is shown  
4 in Fig. 10.  
5  
6

7  
8 Different ceramics were added to the solubilised polymer, to withstand if the interconnecting  
9 layer in the sandwich structure maintains cohesion while processing the hydrogel. The  
10 swelling of the PVA central layer allows interaction between both polymers carrying the  
11 ceramics + drug. As the F/T cycles continue, crosslinking between both polymers occurs at  
12 the PVA interface along with the increase in crosslinking on both polymers.  
13  
14

15 The polymer investigated in this study were PVA and PAA cryogels, which have the  
16 advantages of relatively ease to manufacture and not requiring additional crosslinking  
17 agents. The ceramic component used contains  $\beta$ -TCP, wWollastonite and talc,  $\beta$ -TCP, where  
18  $\text{Ca}^{2+}$  is partially substituted with  $\text{Mg}^{2+}$  ( $\text{Ca}_{2.81}\text{Mg}_{0.19}(\text{PO}_4)_2$ ), wollastonite 2M ( $\text{CaSiO}_3$ ) and  
19 were investigated before by our group showing positive results for bone regeneration and  
20 drug delivery applications [23]. Titanium oxide, rutile  $\text{TiO}_2$  in nanopowder form has been  
21 selected due to its properties in controlled drug release and target drug delivery. The  
22 concentration used in the solubilised polymer for both ceramics, 75% (wt.%), was the  
23 maximum that could be achieved without precipitate. The principle of maximum  
24 concentration was that at maximum concentration the polymer could have been affected at  
25 the point where minimum interaction would occur from the two independent mixed polymers  
26 in the mould. The xerogel was obtained after five F/T cycles and although, it is possible to  
27 obtain different thickness of the PVA layer, we decided to use the thinnest since this  
28 configuration would allow a better interaction between both polymers and reduce any  
29 properties that could be reduced due to the xerogel PVA.  
30  
31  
32  
33  
34  
35  
36  
37  
38  
39  
40  
41  
42  
43  
44  
45  
46  
47  
48  
49  
50  
51  
52  
53  
54  
55  
56  
57  
58  
59  
60

The morphology of the composites examined under SEM in dehydrated form exhibit a well-known porosity and the PVA dried wall shows different characteristics depending on the orientation. The vertical layer seems to be slightly distorted and tortuous, which may be due to the swelling effect when preparing the samples; the interaction where the PVA dried wall comes in contact with the solubilised polymer, when preparing the samples, is higher than the horizontal layer. In addition, since the PVA xerogel was very thin - its mechanical properties are poor, leading to a weak barrier that might deform when preparing the samples. However, both orientations should not exhibit many differences on general properties since the structure is not altered. The effect of aggregation on  $\beta$ -TCP occurs due to the particle sizes (100-300  $\mu\text{m}$ ) been previously reported [23]. The discontinuity on the PVA wall occurs due to the swelling effect owing to the thickness and instability of the hydrogel. Consequently it blends in between the polymers - this effect might not occur with a thicker walled structure.

The structural differences in the FTIR spectra showed that PVA samples with  $\beta$ -TCP influences the adhesion in the hydrogels, which leads to reinforcement of inter-molecular and intra-molecular bonds. With a higher concentration of the ceramics, more bonds are formed reinforcing the structure of the composite. Nonetheless,  $\text{TiO}_2$  indicates only additional peaks corresponding to Ti bonds; although, they are incorporated in the hydrogel as observed in the SEM images. The addition of PAA enhances the inter-molecular bonding through formation of cyclic carboxylic acid dimers – region of  $1700 \text{ cm}^{-1}$  [34]. Usually, formation of new intra-molecular bonds between the oxides and the carboxylic group of PAA occurs at the expense of the cyclic dimers. The variation of the M.W. on PAA seems to maintain the same structural bonds between the oxides and the polymer. However, when examining the double-layered hydrogels, the middle interface of the xerogel, corroborates the proposed method described in Fig 9 where both oxides can be found in this region. However, it is challenging to analyse the intensity of these bonds. Swelling analysis tests with dye exhibits little

1 diffusion between the polymers, this indicates that a good barrier has been formed.  
2 Additionally to allowing a support for both polymers, the hydrogels can deliver the drug  
3 without diffusing to the other polymer side which could change the release rate.  
4  
5  
6  
7  
8  
9

10 No visual differences were observed between the different configurations showing a similar  
11 swelling profile for the different geometries, possibly because the resulting areas that both  
12 polymers interact are similar. The swelling ratios for PVA samples with the addition of  
13 ceramics exhibited a slightly reduction in swelling.  
14  
15  
16  
17  
18  
19

20 With the addition of PAA the samples had an overall increase in swelling and this behaviour  
21 is indicative of the pH sensitivity of the acrylates in PAA, since the swelling test was  
22 performed at pH 7.4, which is facilitated by the dissociation of carboxylic acid groups. The  
23 dissociated groups cause water penetration into the hydrogel and swelling occurs [35].  
24 Furthermore, the increased concentration of the ceramics tends to decrease the swelling due  
25 to the increase in inter and intra molecular bonds. However, we found that the M.W. of the  
26 PAA has little effect on the swelling ratio for the ceramics. Layered hydrogels exhibits the  
27 swelling properties of both ceramics.  
28  
29  
30  
31  
32  
33  
34  
35  
36  
37  
38

39 The drug releases tests were studied using theophylline and a limitation onto this study is that  
40 on double layered samples, the drug was added onto each layer individually, this was done  
41 because there could be interference of the two drugs to study the diffusion. Drug release  
42 studies demonstrate a different release profile for composite hydrogels. PVA samples had a  
43 release similar to both bilayer and monolayer hydrogels with increasing rate of drug  
44 compared to PVA alone. However, when PAA is introduced into the structure, the M.W. is an  
45 important factor for layered structure. This may have occurred because low molecular weight  
46 might reduce the inter + intra molecular bonding. Nonetheless, the increase in molecular  
47 weight of PAA increases the crosslinks between the polymer chains on F/T technique [7]; this  
48  
49  
50  
51  
52  
53  
54  
55  
56  
57  
58  
59  
60

leads to a very similar profile of controlled release to all different concentrations with these polymers. These profiles are potentially choices for optimum controlled drug, as both layers can deliver different drugs in a similar rate.

Rheological measurements were used to compare the strength of the different composites. It is possible to obtain the storage modulus with this technique, which measures the recoverable energy and the ability to recover following strain. Storage modulus is dependent on the level of crosslinking in a system. The introduction of ceramics, improves the storage modulus and the addition of PAA varies depending on the molecular weight. Introduction of the low molecular weight decreases the crosslinking and consequently reduces the storage modulus. As the molecular weight increases, more crosslinking occurs and strong materials can be formed leading to more inter- and intra-molecular bonding as observed from the FTIR spectra. In addition, due to the high concentration of the ceramics, it tends to increase the storage modulus not only for  $\beta$ -TCP but also for  $TiO_2$ . For bilayer hydrogels, their profiles indicated the incorporation of both structures. Frequency-sweep exhibited that most of the composites studied in this work behaves like a solid indicated by the linear storage modulus response. In addition, frequency-sweep shows similar results from the strain-sweep tests.

The double layered composite with addition of ceramics can not only benefit the biocompatibility but also improve the mechanical properties, which suggest that this material has potential in bone regeneration applications while also being able to control independently, for each layer, the release of complex dual drugs and/or acting as an anti-infection barrier. The constructions of these hydrogels are simple and can be investigated, in future work, via the addition of more layers while also altering the proportion of the composites/drug for a specific drug delivery. In addition, the separation of the layers by the xerogel following the F/T process provides a very good crosslink between the two layers

which can be further investigated in terms of the localised strength of this xerogel between the composites.

## 5. Conclusion

In this work, we evaluated a layered composite of PVA/PAA cryogels that could be used for bone healing and drug delivery. We found that the layered structured composed of a PVA xerogel can indeed act as a barrier and crosslink between both polymers with ceramics as confirmed by FTIR and SEM. The ceramic can enhance the mechanical properties of the composite within the hydrogel while also delivering a drug independently from each layer. The pH sensitivity of this composite was confirmed via swelling and the profile of both ceramics was obtained with similar results on rheology tests. We believe that the approach outlined has enormous potential in that layers and hydrogels can be tailored for specific drugs and drug release profiles.

## Acknowledgements

This work was supported by research grants from science without borders and Capes and NEW GEN (MP1301) Biomimetic and Customized Implants for Bone Engineering COST Action Short Term Scientific Mission.

## References

- [1] T.M.R. Miranda, A.R. Gonçalves and M.T.P. Amorim, *Polymer International*, 2001, **50**, 1068.
- [2] H. Bai, J. Xu, Y. Zhang, X. Liu and O.J. Rojas, *Journal of Polymer Science, Part B: Polymer Physics*, 2015, **53**, 345.
- [3] O. Okay, 2014.
- [4] C.M. Hassan, and N. a. Peppas, *Macromolecules*, 2000, **33**, 2472.
- [5] M.J.D. Nugent, A. Hanley, P.T. Tomkins and C.L. Higginbotham, *Journal of Materials Science: Materials in Medicine*, 2005, **16**, 1149.
- [6] S. Jiang, S. Liu and W. Feng, *Journal of the Mechanical Behavior of Biomedical Materials*, 2011, **4**, 1228.
- [7] M.J. Mc Gann, C.L. Higginbotham, L.M. Geever and M.J.D. Nugent, *International journal of pharmaceutics*, 2009, **372**, 154.
- [8] G.G. De Lima, R.O. De Souza, A.D. Bozzi, M.A. Poplawska, D.M. Devine and M.J.D. Nugent, *Journal of pharmaceutical sciences*, 2015, **105**, 1248.
- [9] G.G. de Lima, D. Kanwar, D. Macken, L. Geever, D.M. Devine and M.J.D. Nugent, in *Handbook of Polymers for Pharmaceutical Technologies*, (Thakur, V. K. & Thakur, M. K.) John Wiley & Sons, Inc., 2015, 1.
- [10] C.M. Hassan, J.E. Stewart and N.A. Peppas, *European Journal of Pharmaceutics and Biopharmaceutics*, 2000, **49**, 161.
- [11] T. Nakajima, N. Takedomi, T. Kurokawa, H. Furukawa and J.P. Gong, *Polymer*

- 1  
2  
3      *Chemistry*, 2010, **1**, 693.  
4  
5  
6 [12] W.K. Wan, G. Campbell, Z.F. Zhang, A.J. Hui and D.R. Boughner, *Journal of*  
7      *biomedical materials research*, 2002, **63**, 854.  
8  
9  
10  
11 [13] H. Du, and J. Zhang, *Soft Matter*, 2010, **6**, 3370.  
12  
13  
14 [14] A. Shirole, J. Sapkota, E.J. Foster and C. Weder, *ACS applied materials & interfaces*,  
15  
16      2016, **8**, 6701.  
17  
18  
19 [15] S. Spoljaric, A. Salminen, N.D. Luong and J. Seppälä, *European Polymer Journal*,  
20  
21      2014.  
22  
23  
24  
25 [16] H. Zhang, H. Xia and Y. Zhao, *ACS Macro Letters*, 2012, **1**, 1233.  
26  
27  
28 [17] C. Curley, J.C. Hayes, N.J. Rowan and J.E. Kennedy, *Journal of the mechanical*  
29      *behavior of biomedical materials*, 2014, **40C**, 13.  
30  
31  
32  
33 [18] U. Fumio, Y. Hiroshi, N. Kumiko, N. Sachihiko, S. Kenji and M. Yasunori,  
34  
35      *International journal of pharmaceutics*, 1990, **58**, 135.  
36  
37  
38 [19] G.G. de Lima, L. Campos, A. Junqueira, D.M. Devine and M.J.D. Nugent, *Polymers*  
39  
40      *for Advanced Technologies*, 2015, **26**, 1439.  
41  
42  
43  
44 [20] P. Taepaiboon, U. Rungsardthong and P. Supaphol, *Nanotechnology*, 2006, **17**, 2317.  
45  
46  
47 [21] S.G. Rathod, R.F. Bhajantri, V. Ravindrachary, J. Naik and D.J.M. Kumar, *RSC*  
48      *Advances*, 2016, **6**, 77977.  
49  
50  
51 [22] J.-T. Zhang, R. Bhat and K.D. Jandt, *Acta biomaterialia*, 2009, **5**, 488.  
52  
53  
54  
55 [23] M. Canillas, G.G. de Lima, M.A. Rodríguez, M.J.D. Nugent and D.M. Devine, *Journal*  
56  
57      *of Polymer Science Part B: Polymer Physics*, 2015, n/a.  
58  
59  
60

- 1  
2 [24] E. Castro, V. Mosquera and I. Katime, *Nanomaterials and Nanotechnology*, 2012, **2**, 1.
- 3  
4 [25] L. Wei, C. Cai, J. Lin and T. Chen, *Biomaterials*, 2009, **30**, 2606.
- 5  
6 [26] B.J. Lee, S.G. Ryu and J.H. Cui, *International Journal of Pharmaceutics*, 1999, **188**,
- 7 71.
- 8  
9 [27] X. Yang, K. Yang, F. Yu, X. Chen, S. Wu and Z. Zhu, *Polymer International*, 2009,
- 10  
11 [28] W. Li, J. Kang, Y. Yuan, F. Xiao, H. Yao, S. Liu, J. Lu, Y. Wang, Z. Wang and L.
- 12  
13 Ren, *Composites Science and Technology*, 2016, **128**, 58.
- 14  
15 [29] F.J. Martínez-Vázquez, A. Pajares, F. Guiberteau and P. Miranda, *Materials*, 2014, **7**,
- 16  
17 4001.
- 18  
19 [30] T. Wang, H. Jiang, L. Wan, Q. Zhao, T. Jiang, B. Wang and S. Wang, *Acta*
- 20  
21 *Biomaterialia*, 2015, **13**, 354.
- 22  
23 [31] H.S. Mansur, C.M. Sadahira, A.N. Souza and A.A.P. Mansur, *Materials Science and*
- 24  
25 *Engineering: C*, 2008, **28**, 539.
- 26  
27 [32] J.J. Maurer, D.J. Eustace and C.T. Ratcliffe, *Macromolecules*, 1987, **20**, 196.
- 28  
29 [33] G. Busca, G. Ramis, J.M.G. Amores, V.S. Escribano and P. Piaggio, *J. Chem. Soc.*
- 30  
31 *Faraday Trans.*, 1994, **90**, 3181.
- 32  
33 [34] D.M. Devine, and C.L. Higginbotham, *Polymer*, 2003, **44**, 7851.
- 34  
35 [35] D.M. Devine, and C.L. Higginbotham, *European Polymer Journal*, 2005, **41**, 1272.

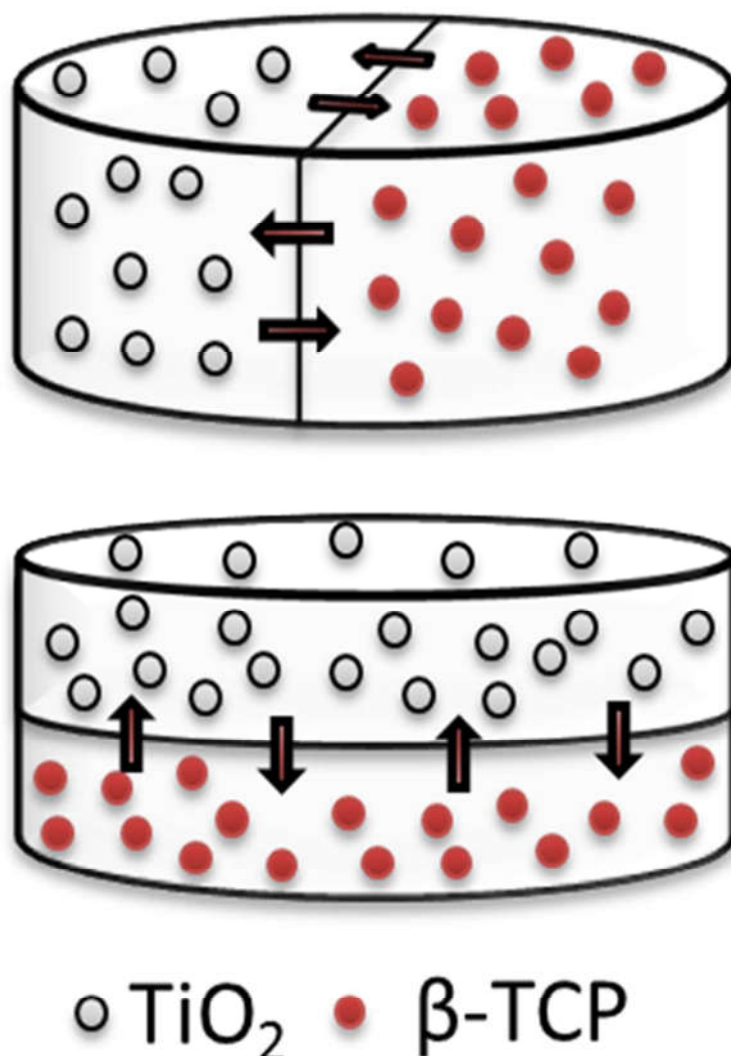


Figure 1. Schematic representation of both geometries used in this work.

Fig. 1

52x79mm (300 x 300 DPI)

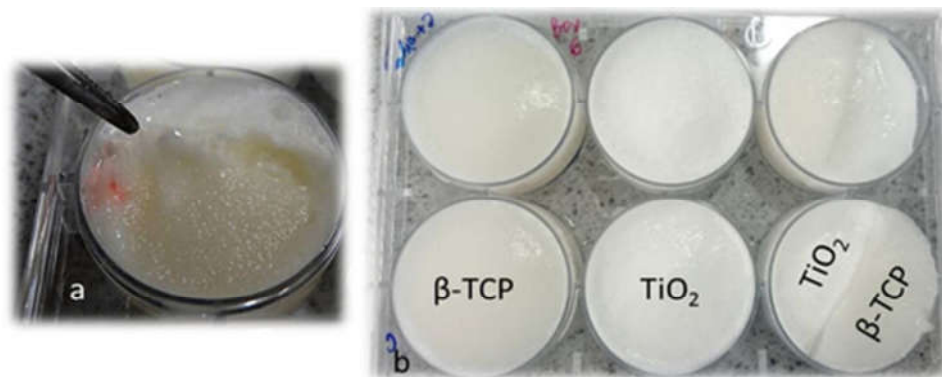


Figure 2. a) Crosslinking between the xerogel and the two different hydrogels after one cycle of F/T. b) PVA samples with ceramics analysed in this work following four F/T cycles.

Fig.2  
41x16mm (300 x 300 DPI)

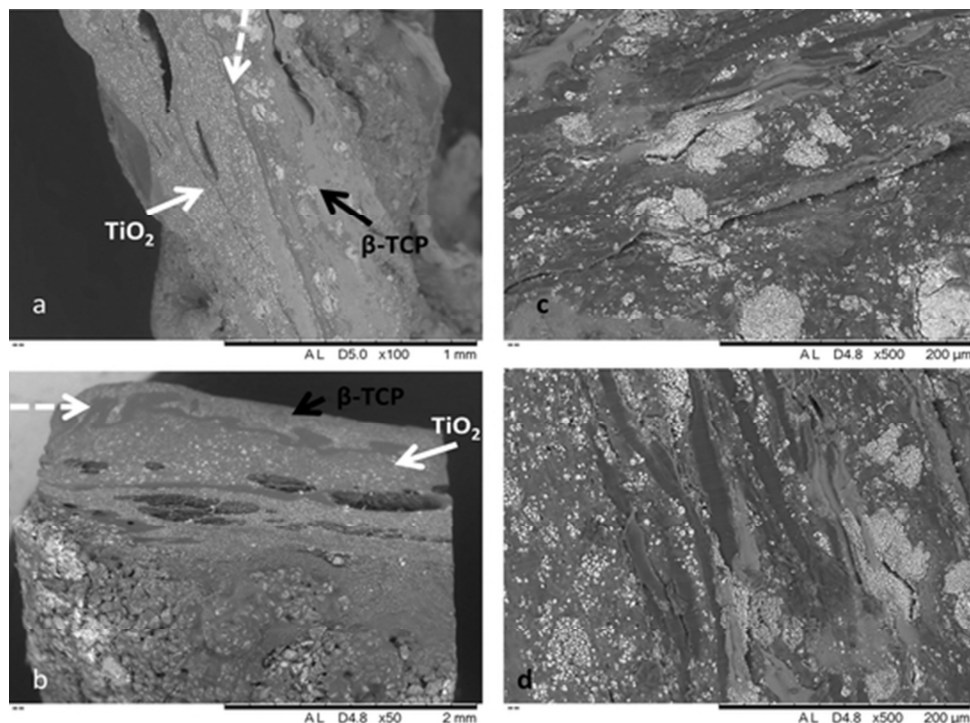


Figure 3. Horizontal layer detailed region at (a) 100x and (c) 500x. Vertical layer detailed region at (c) 50x and (d) 500x. Dashed arrows indicate the xerogel location.

Figure 3  
46x34mm (300 x 300 DPI)

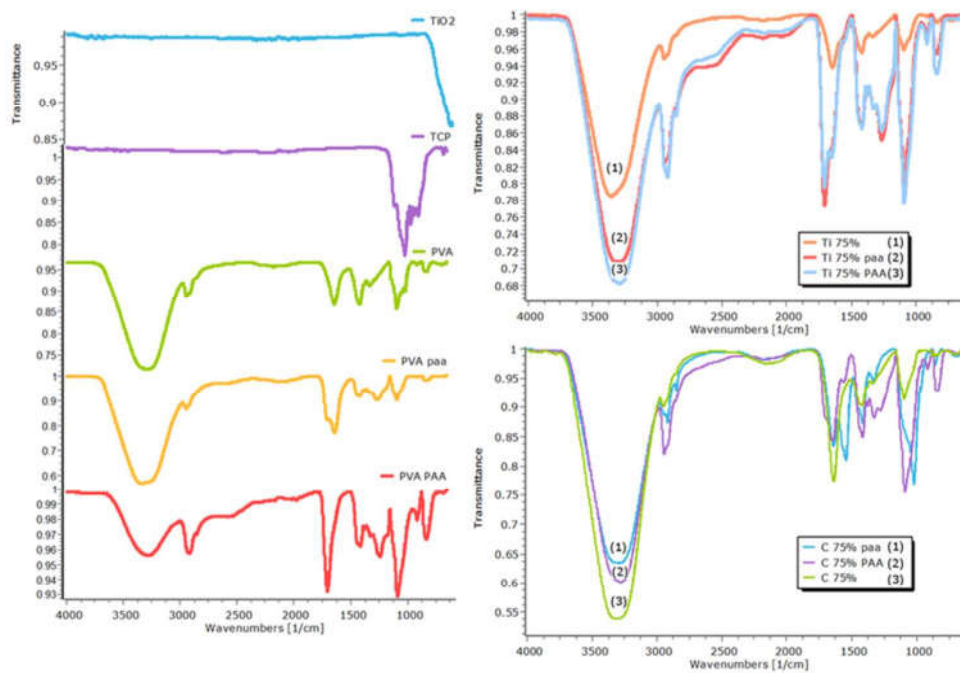


Figure 4. FTIR spectra of the different studied samples: (a) PVA (b) PVA + paa (low molecular weight) and (c) PVA + PAA (high molecular weight).

Fig 4

72x50mm (300 x 300 DPI)

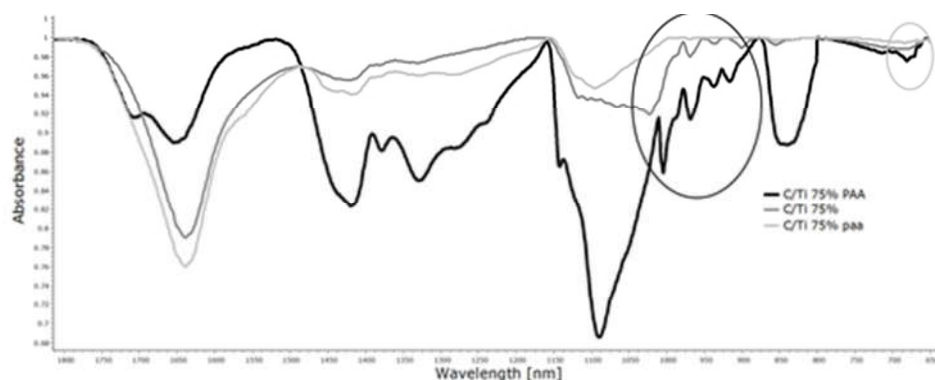


Figure 5. FTIR detailed region for the layered composite hydrogels. Circle area indicates the peaks corresponding to  $\beta$ -TCP and TiO<sub>2</sub>. Black and grey circle area indicates  $\beta$ -TCP and TiO<sub>2</sub> respectively.

Fig.5

46x18mm (300 x 300 DPI)

1  
2  
3  
4  
5  
6

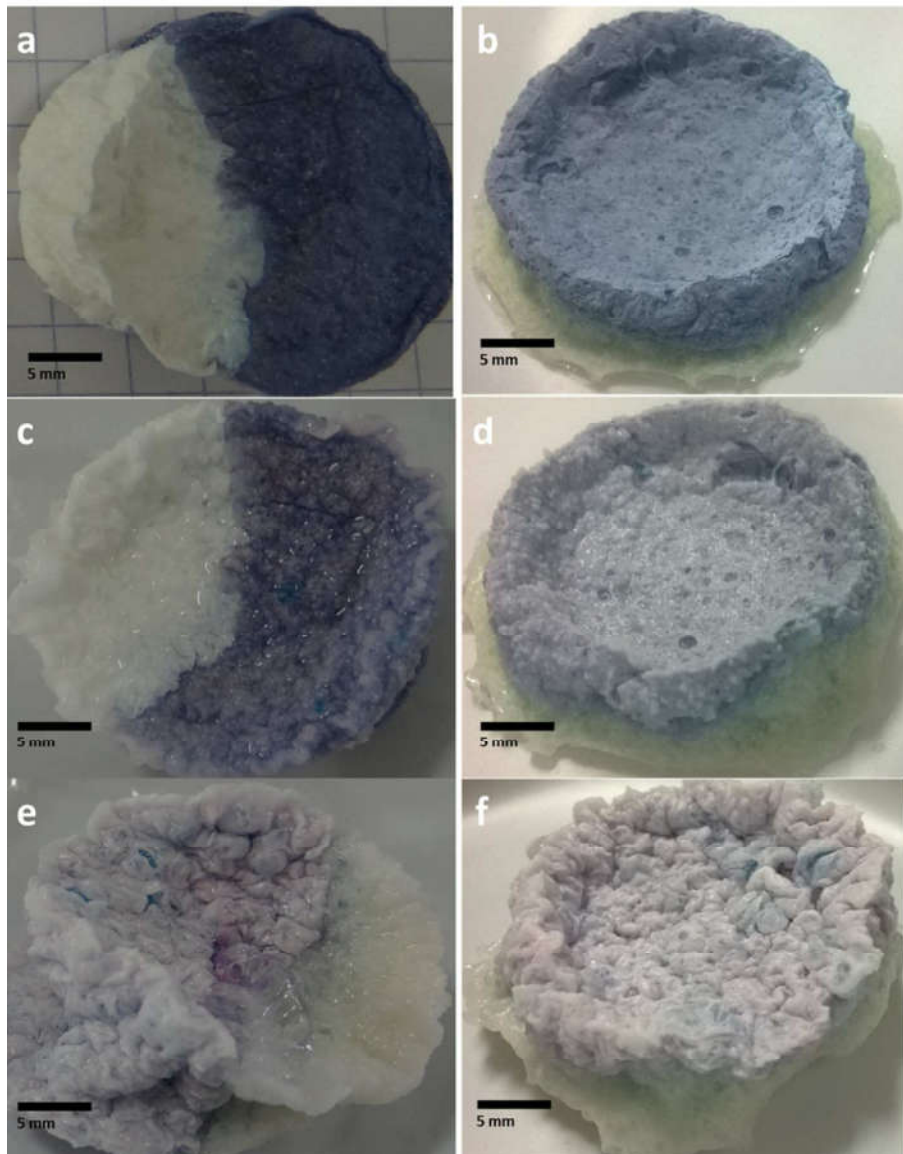


Figure 6.  $\beta$ -TCP/TiO<sub>2</sub> PVA/PAA hydrogels dried samples before swelling. (a,b); swelling after 30 min (c-d) and 12 h (e-f) in PBS pH 7.4; (a-c-e) Vertical division, (b-d-f) horizontal division.

Fig.6

73x94mm (300 x 300 DPI)

46  
47  
48  
49  
50  
51  
52  
53  
54  
55  
56  
57  
58  
59  
60

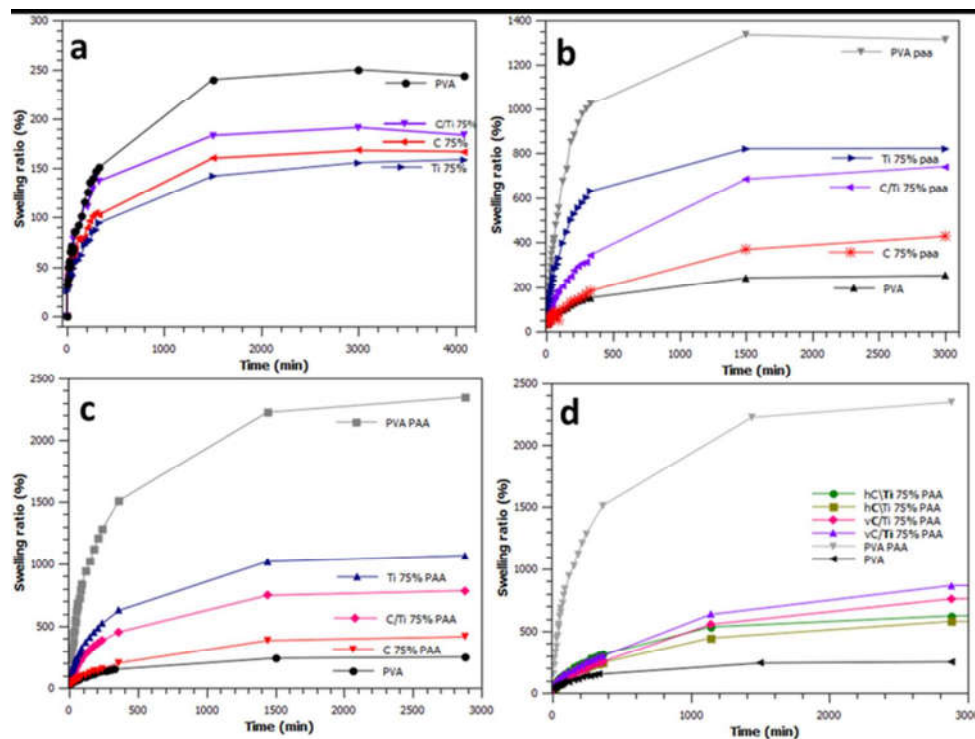


Figure 7. Swelling profiles of (a) PVA, (b) PVA + paa (low molecular weight), (c) PVA + PAA (high molecular weight) and (d) PVA + PAA dye samples.

Fig.7  
65x49mm (300 x 300 DPI)

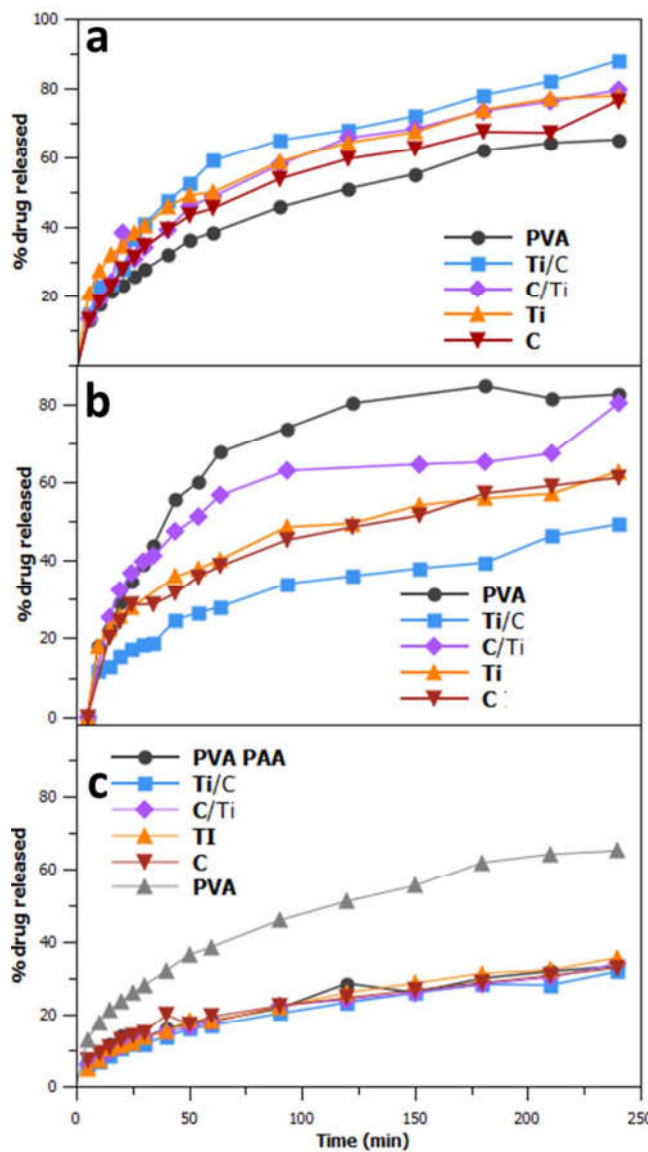


Figure 8. Drug release profiles of the studied samples a) PVA; b) PVA + paa and c) PVA + PAA. Bold characters indicate where the drug has been loaded.

Fig.8  
80x145mm (300 x 300 DPI)

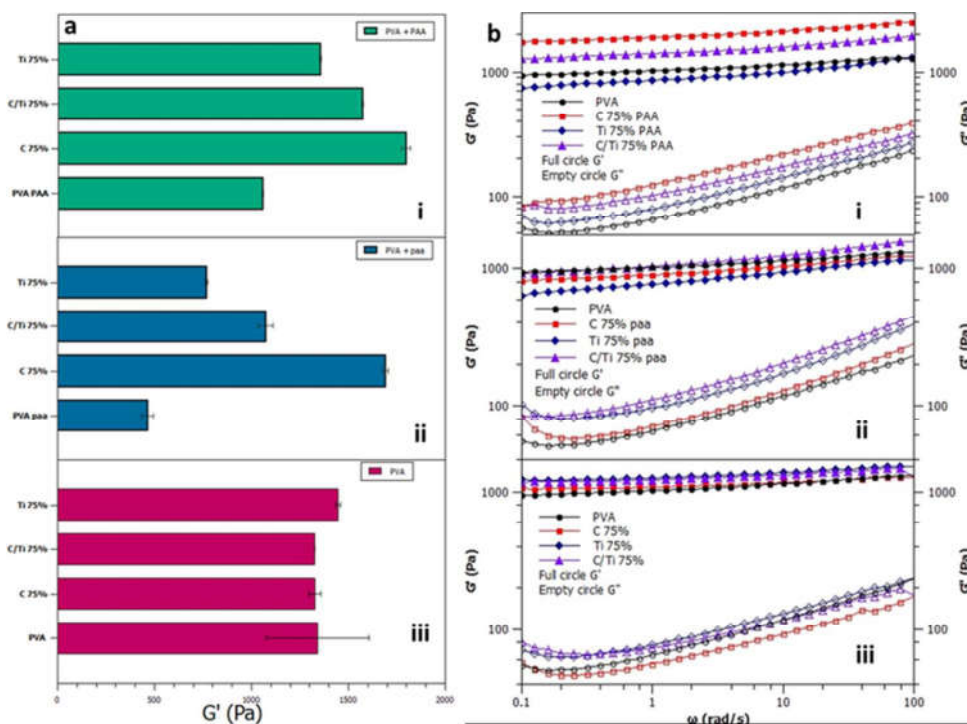


Figure 9. Rheology results of studied samples, i) PVA + PAA; ii) PVA + paa; iii) PVA. (a) Strain-sweep and (b) Frequency dependence of  $G'$  and  $G''$  for the different composite cryogels - PVA ( $\bullet G'$ ,  $\circ G''$ ), Ceramic -  $\beta$ -TCP ( $\blacksquare G'$ ,  $\square G''$ ), Ti - TiO<sub>2</sub> ( $\blacklozenge G'$ ,  $\diamond G''$ ) and C/Ti - Double layer ( $\blacktriangle G'$ ,  $\triangle G''$ ).

Fig.9

64x47mm (300 x 300 DPI)

1  
2  
3  
4  
5  
6  
7  
8  
9  
10  
11  
12  
13  
14  
15  
16  
17  
18  
19

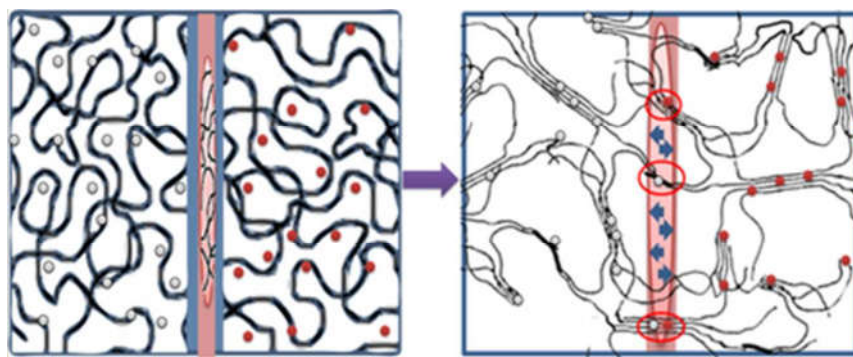


Figure 10. Purposed method of bilayer synthesis cryogels. Solubilized polymer crosslinks after F/T process and ceramics/drugs becomes entrapped between the chains, the xerogel swells in between the F/T cycles which allow bonding between both layers of the studied composite.

Fig. 10

37x15mm (300 x 300 DPI)

20  
21  
22  
23  
24  
25  
26  
27  
28  
29  
30  
31  
32  
33  
34  
35  
36  
37  
38  
39  
40  
41  
42  
43  
44  
45  
46  
47  
48  
49  
50  
51  
52  
53  
54  
55  
56  
57  
58  
59  
60